Why not record from *every* channel with a CMOS scanning probe?

George Dimitriadis[1, *], Joana P. Neto[1, 8, 18, *], Arno Aarts[2], Andrei Alexandru[3], Marco Ballini[3], Francesco Battaglia[4], Lorenza Calcaterra[1], Francois David[5], Richárd Fiáth[6, 7], João Frazão[8], Jesse Geerts[1], Luc J. Gentet[5], Nick Van Helleputte[3], Tobias Holzhammer[2], Chris van Hoof[3], Domonkos Horváth[6, 7, 9], Gonçalo Lopes[1], Eric Maris[4], Andre Marques-Smith[1], Gergely Márton[6, 7], Domokos Meszéna[6, 7], Srinjoy Mitra[10], Silke Musa[3], Hercules Neves[11, 17], Joana Nogueira[1], Guy A. Orban[12], Frederick Pothof[13], Jan Putzeys[3], Bogdan Raducanu[3, 14], Patrick Ruther[13], Tim Schroeder[4], Wolf Singer[15], Paul Tiesinga[16], Istvan Ulbert[7, 6], Shiwei Wang[3], Marleen Welkenhuysen[3], Adam R. Kampff[1]

1) Sainsbury Wellcome Centre for Neural Circuits and Behaviour, University College London, United Kingdom
2) ATLAS Neuroengineering, Leuven, Belgium
3) Life Science Technologies Department, IMEC, Belgium
4) Donders Institute for Brain, Cognition and Behavior, Radboud University Nijmegen, The Netherlands
5) Team Waking, Lyon Neuroscience Research Center (CNRL), INSERM-U1028, CNRS-UMR5292, Bron, France
6) Institute of Cognitive Neuroscience and Psychology, Research Centre for Natural Sciences, Hungarian Academy of Sciences, Budapest, Hungary
7) Faculty of Information Technology and Bionics, Pazmany Peter Catholic University, Budapest, Hungary
8) Champalimaud Neuroscience Programme, Champalimaud Centre for the Unknown, Portugal
9) School of PhD Studies, Semmelweis University, Budapest, Hungary
10) Institute for Integrated Micro and Nano Systems (IMNS), University of Edinburgh, UK
11) Uppsala University, Sweden
12) Department of Medicine and Surgery, University of Parma, Parma, Italy
13) Department of Microsystems Engineering (IMTEK), University of Freiburg, Germany
14) Katholieke Universiteit Leuven, Belgium
15) ErnstStrüngmann Institute for Neuroscience in Cooperation with Max Planck
16) Neurinformatics department, Donders Institute for Brain, Cognition and Behavior, Radboud University Nijmegen, Heyendaalseweg 135, 6525 AJ, Nijmegen, The Netherlands
17) Fiocruz, Brazil
18) Departamento de Ciência dos Materiais, CENIMAT/I3N and CEMOP/Uninova, Faculdade de Ciências Tecnologia−Universidade Nova de Lisboa, Caparica, Portugal

Abstract

Neural recording devices normally require one output connection for each electrode. This constrains the number of electrodes that can be accommodated by the thin shafts of implantable probes. Sharing a single output connection between multiple electrodes relaxes this constraint and permits designs of ultra-high density neural probes.

Here we report the design and *in vivo* validation of such a device, a complementary metal-oxide-semiconductor (CMOS) scanning probe with 1344 electrodes and 12 reference electrodes along an 8.1 mm x 100 µm x 50 µm shaft; the outcome of the European research project NeuroSeeker. This technology presented new challenges for data management and visualization, and we also report new methods addressing these challenges developed within NeuroSeeker.

Scanning CMOS technology allows the fabrication of much smaller, denser electrode arrays. To help design electrode configurations for future probes, several recordings from many different brain regions were made with an ultra-dense passive probe fabricated using CMOS process. All datasets are available online.

Introduction

The number of neurons that can be monitored simultaneously during an extracellular recording is currently limited by the number of electrodes that can be implanted (Stevenson & Kording 2011; Stevenson 2017). However, the desire for large-scale monitoring of neural activity and the need to minimize tissue damage compete with one another (Buzsáki et al. 2015) The high resolution processes of semiconductor fabrication (i.e., photolithographic patterning of thin film conductors and insulators on a silicon substrate) have enabled dozens of microelectrodes, packed with an ever increasing density, along needle-like probes (Berényi et al., 2014; Blanche, 2005; Buzsáki et al., 2015; Du et al., 2011; Shobe et al., 2015; Torfs et al., 2011). In the standard “passive” silicon probe, electrodes distributed along the probe shaft must each be connected to an external contact pad on the probe base by metal lanes deposited along the shaft. Advances in lithography techniques (i.e., e-beam lithography (Rios et al. 2016; Scholten & Meng 2016)), metal deposition procedures, and quality control have made it possible to fabricate a five shank, 1000-channel probe, where each shank (width of ~50 µm) has 200 electrodes of 9 × 9 µm and a pitch of 11 µm (Scholvin et al. 2016). Despite these impressive designs, a bottleneck remains in the number of output connection lanes that can be squeezed into the thin probe shaft. Therefore, monitoring the thousands of electrodes required to densely cover an 8 mm x 100 µm probe will require a new technology; a technology that multiplexes the signal from multiple electrodes into one output lane.

The semiconductor industry has solved the same interconnect challenge with integrated circuitry (IC), often fabricated using the CMOS process. As a characteristic example, mobile phones with on board cameras use CMOS image sensors (CIS) that are lightweight and low power, but that can convert an optical image into an electronic signal with very high spatial resolution. A CIS is composed of an array of millions of identical pixels, each having at least a photodiode, an addressing transistor that acts as a switch, and an amplifier. Each pixel is sampled once within each frame and the image output is generated by rapidly scanning the full sensor matrix. This active switching / time multiplexing is crucial for achieving the small size of a CIS device, as it conveys the signals from many pixels with just a few output connections.

In the case of silicon probes, their 1D physical architecture and high sampling speed requirements have challenged the inclusion of integrated circuitry on the probe's shaft. Although the concept of integrating electronic elements in the shank of a neural probe was first introduced in the 1980s (Kensall and Wise, 1992; Najafi and Wise, 1986; Najafi et al., 1985; Wise and Najafi, 1991) the silicon probe fabrication has only recently evolved to achieve integrated circuits in the same substrate used to build the recording electrodes. The most recent CMOS-based implantable probe designs for *in vivo* applications integrate circuitry into both the probe base and within the probe shaft(s) and have been reviewed elsewhere (Obien et al. 2015; Ruther & Paul 2015; Seymour et al. 2017; Lopez et al. 2013; Lopez et al. 2016; Steinmetz 2016; Raducanu et al. 2016).

The NeuroSeeker European research project aimed to produce CMOS-based, time multiplexing, silicon probes for extracellular electrophysiological recordings with 1344 electrodes on a 50 µm thick, 100 µm wide, and 8 mm long shank with a 20 x 20 µm electrode size and a pitch of 22.5 µm (see Box 1 for a technical overview of the probe and (Raducanu et al. 2016; Raducanu et al. 2017) for an in depth description of the probe's design). This innovative solution has allowed the neuroscientists within the consortium to record brain activity with an unprecedented combination of resolution and scale. Here we report the use of the NeuroSeeker probe to record from both anesthetized and freely moving rats. We characterize in saline and *in vivo* the increase in noise that the local amplification and time multiplexing scheme incurs relative to a passive electrode probe with the same configuration. We show that this increase is insignificant *in vivo* and does not inhibit the capture of high quality neural signals. In the case of freely moving animals, we also include proof-of-concept data that the signal remains stable for at least 2 weeks, and describe a method for removing the NeuroSeeker probe intact, and ready for reuse, from the brain of a chronically implanted animal. This allows the multiple re-use of probes whose price, and low production numbers, makes them currently inaccessible to all but a tiny minority of electrophysiology labs around the world.

Recording with this number of electrodes results in datasets of around 200 GB per hour with spike numbers in the millions. This scale of data poses new difficulties in the visualization, curation, and pre-processing of the signal, even before it can be used to explore correlations with sensory stimuli or behaviour. Here we present an online visualization method that allows for the rapid overview of the signal from all 1344 electrodes, giving the experimenter a global picture of the recording quality as it is taking place.

Given that CMOS probes with local amplification and time multiplexing allow a significant increase in electrode density without sacrificing compactness, the neuroscientific community must now determine the physiologically relevant limit for the size and density of the electrodes on such probes. To help address this question, we have collected datasets from ultra-high density (256 electrodes of 5 x 5 µm size with a 6 µm pitch) passive probes. These were recorded from anesthetized rats in a wide range of brain structures and probe orientations. These datasets are available online for further analysis of the optimal geometries for future CMOS probes.

Box 1. NeuroSeeker CMOS-based probe.

The NeuroSeeker probe contains 1344 small electrodes (20×20µm) with 2.5µm spacing and 12 larger reference electrodes (40 × 80 µm).

Time division multiplexing within the shank allows 8 electrode outputs on a single output connection. If a single metal line can be shared by several electrodes, we are no longer restrained by the number of metal lines that can fit within the cross-section of a shank or by the size of the bonding interface in the probe base.

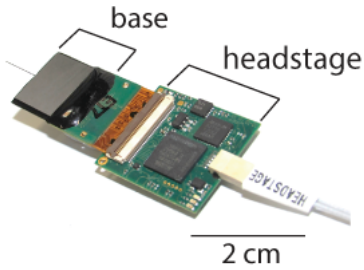

The challenge in such a design is that each electrode requires its own amplifier and active switching circuit positioned directly underneath it. The amplifier is needed since the high impedance electrode cannot by itself drive the multiplexed readout lines at sufficient speed (Obien et al., 2015)

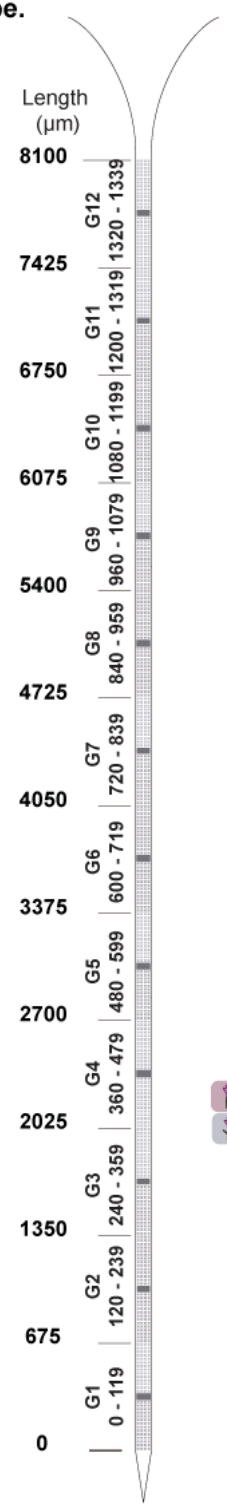

Basic principle of time division multiplexing

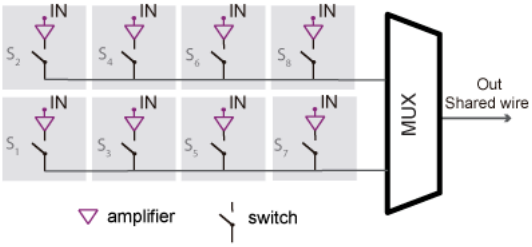

The current is integrated for a fixed period of time (Ti = 2.5 µs) over a capacitor (Ci = 15 pF) shared among 8 channels in the probe base. After Ti, the voltage on Ci is sampled and then it is discharged for the next cycle. The integration reduces out-of-band noise, acting as anti-aliasing filter. Each channel is oversampled at fs = 40 kHz (neural signal band is limited to ~ 7.5 kHz, therefore fs > 15 kHz), producing a total multiplexing frequency of 320 kHz. The signal is fed to an integrator, in the base, whose output is demultiplexed (DMUX block).

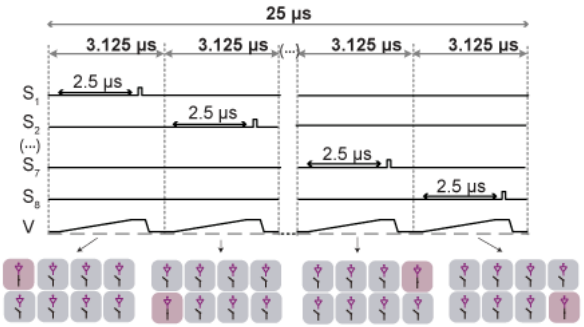

Each reference electrode is made from a bin of 8 electrodes, therefore the circuit handles, in total, 1440 channels. A total of 180 Integrator-DMUX blocks drive the 1440 channels, which are further amplified and filtered on the base, keeping only the band of interest. These signals are then multiplexed and digitized in groups of 20 channels (10-bit successive approximation analog-to-digital converter) by 72 ADCs. Finally, a digital control block is responsible for generating the clocks for the ADCs and the MUX/DMUX blocks. It also serializes the parallel data from all the ADCs to only 6 data lines (Raducanu et al., 2016).

Results

Several recordings were performed with the NeuroSeeker CMOS-based scanning probes *in vivo* to evaluate the viability of these devices. There are 12 groups of electrodes on the probe, which can be individually powered, labelled from G1 to G12, in Box 1 and Figure 1. Each group contains 120 channels: 112 electrodes and 1 local reference in the middle made from a group of 8 electrodes binned together. For each electrode, the user can select the reference type (external or internal), gain, and frequency bandwidth (high-pass cut-off frequency in AP mode or low-pass cut-off frequency in LFP mode). For all recordings, 1277 electrodes were set in the AP band (0.5–7.5 kHz), while 67 were set in the LFP band (1-500Hz). The LFP electrodes were spaced 20 electrodes apart from one another, which translates to 5 rows, or, given the 22.5 µm pitch of each electrode, 112.5 µm.

Neural recordings

Figure 1A shows a representative epoch of a recording performed simultaneously within cortex, hippocampus, and thalamus from an anesthetized rat. In this recording, 10 of the 12 groups are in the brain and thus enabled (powered on): 1060 out of the 1120 electrodes are set in AP mode with 60 set to LFP mode. A subset of traces from electrodes set in AP and LFP mode are shown in Figure 1A (a complete record of all traces is shown in Supplementary Figure 1). The traces in AP mode are displayed in groups (c1, c2, c3, cg, h1, h2, h3, h4, t1, t2, t3 and t4) that corresponds to the location on the probe shaft indicated by the black region in the probe schematic. Moreover, traces of 11 out of 60 LFP mode electrodes are plotted between the group traces. The presence of fast voltage deflections in several traces reveals that the spiking activity of multiple neurons has been detected. Furthermore, the NeuroSeeker probe densely samples the local electric field, providing a detailed description of the spatiotemporal profile of a neuron's extracellular action potential as shown in Figure 1C.

To evaluate if the data quality deteriorates with increasing number of groups powered, we computed the noise of 212 electrodes (from groups G1 and G2) set in AP mode while enabling more groups along the shank. The noise level for the 212 electrodes using the external reference, with 2 groups and 12 groups powered, is 10.2 ± 0.1 µV and 12.0 ± 0.1 µV, respectively. Additionally, the noise magnitude was computed for the 1012 channels in the brain (half of group 10's electrodes are outside of the brain) using either the external or the internal reference configuration while recording. The measured noise using the external and internal reference is 11.7 ± 0.1 µV and 12.5 ± 0.1 µV, respectively. The noise magnitude computed across these datasets revealed no significant variability. We also measured the noise in saline for the NeuroSeeker probe. The measured noise in saline while powering the same 1012 channels was 9.4 ± 0.1 µV. We compared the noise measured in saline and during acute recordings with a 128-channel probe previously described (Neto et al., 2016). This passive electrode probe has the same configuration, electrode size, and electrode material (titanium nitride) as the CMOS based probe (impedance at 1 kHz is around 50 kOhm). The noise value calculated with the 128-channel probe in saline was 2.69 ± 0.02 µV and *in vivo* (*amplifier2015-08-28T20_15_45* in http://www.kampff-lab.org/validating-electrodes/) was 10.40 ± 0.04 µV. Despite the difference in saline (9.4 vs 2.7 µV) the noise difference *in vivo* was small (11.7 vs 10.4 µV) between the CMOS based probe and the passive 128-channel probe, highlighting the dominance of "biological" noise for *in vivo* extracellular recording.

Several recordings were performed with different reference configurations and number of active groups. These datasets are available online (http://www.kampff-lab.org/cmos-scanning/) and

summarized in Supplementary Table 1. Figure 1 is derived from one of these recordings, *18_26_30.bin*.

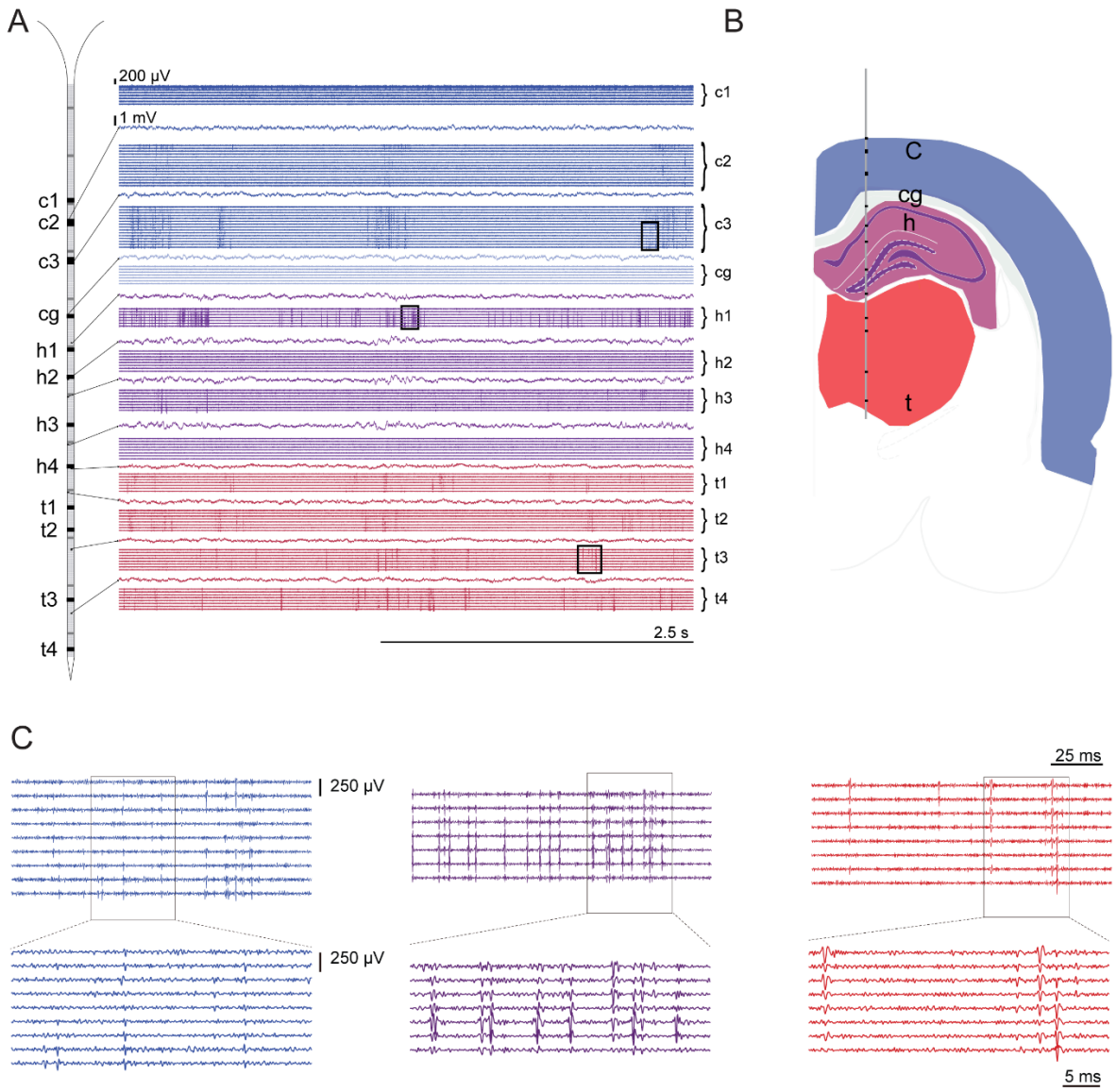

Figure 1. Example of a recording performed with 1120 electrodes simultaneously within cortex, hippocampus, and thalamus from an anesthetized rat. A) 5-s-long LFP and AP traces of a probe spanning multiple brain regions; B) Schematic of coronal slice indicating each group's position in A as black blocks. 'c, 'cg', 'h' and 't' denote the anatomic locations of cortex, cingulum, hippocampus, and thalamus, respectively. The estimated probe position was based on the insertion coordinates and physiological signatures. From the point of insertion to the tip, the recording length was 6.7 mm; C) Short epochs of AP band traces from groups c3, h1, and t3 (color-coded), illustrating the presence of diverse spike waveforms on several electrodes. These sections are highlighted in A by boxed areas on top of each trace.

We also conducted a set of recordings from a chronically implanted animal. The recordings lasted for 15 days following surgery, at which point the recording chamber became unstable. The implant had all 12 groups inserted in the brain and all of them were enabled, thus recording from 1277 AP and 67 LFP small electrodes. These results are preliminary (Supplementary Figure 2), but demonstrate proof-of-concept viability for monitoring neural activity over two-weeks.

Given the high costs and low availability of high density probes, we designed a method that allowed us to extract the CMOS probe from the brain of a chronically implanted animal at the end of the experimental period so that it can be reused for multiple experiments. This required a specially designed probe holder and a series of steps after animal euthanasia to ensure the probe is removed without breaking the fragile shaft. The holder is a two-part design and is shown in Supplementary Figure 2a, along with detailed probe recovery methods.

Data visualization

The signal traces presented in Figures 1 are just a small fraction of the total number of electrodes (105 of 1060 electrodes) recorded during an acute experiment (see all voltage traces in Supplementary Figure 1). These ultra-high channel count CMOS scanning probes presented a new challenge for the presentation and analysis of the acquired data. This challenge first appears when the user wants to monitor an ongoing recording, either to assess the signal quality appearing on each electrode or to better position the probe within the desired brain structure(s). Visualizing 1344 timeseries is difficult, even on an HD monitor with only 1080 rows of pixels. Furthermore, rendering voltage vs. time traces, the conventional representation for online physiology signals, is computationally expensive. However, modern graphic processors (GPUs) were specifically designed to parallelize such visualization tasks. We therefore developed a custom visualization pipeline using Bonsai (Lopes et al. 2015) by transferring each buffer of acquired probe data directly to the GPU and then using fragment shaders to render all probe data in real-time. The visualization shown in Figure 2 is a screen capture of one such online visualization in which the voltage signal of each channel is rendered from red to blue (also see Supplementary movie 1). A neuron's extracellular action potential is detected on many adjacent electrodes, and thus spikes in this visualization appear as a coloured block of red and blue stripes.

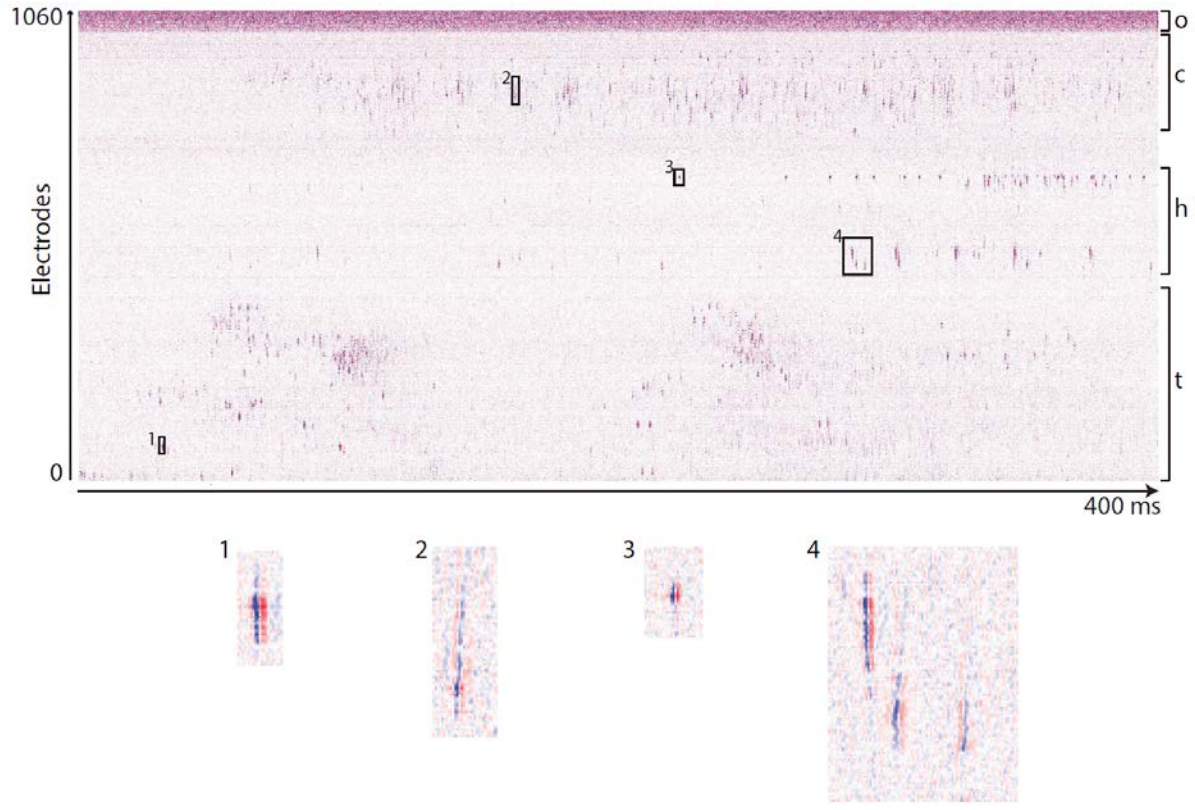

Figure 2. Realtime GPU-based visualization of the voltage traces from all (1060) electrodes in AP mode during acute recordings under anesthesia. The voltage traces recorded by each electrode (row) are displayed as a color saturation for each 100 microsecond bin (column). Red represents positive voltages, blue negative voltages, and white represents voltages near zero. This image shows 400 milliseconds of data recorded simultaneously in cortex, hippocampus and thalamus. 'o': out of the brain, 'c': cortex, 'h': hippocampus and 't': thalamus.

Do we need all these electrodes?

Integrating CMOS-based scanning technology into the shaft of an *in* vivo neural probe has now made it possible to drastically increase electrode density. However, given the challenges associated with the volume of data generated by such probes, neuroscientists must decide whether further increases in recording density are actually useful. Current approaches to spike sorting would appear to benefit from higher density probes (Dimitriadis et al. 2016; Moore-Kochlacs 2016; Rossant et al. 2015). Furthermore, initial results (J. Jun et al. 2017) show that increased electrode densities could help compensate for drift in chronic recordings and allow following individual neurons over the course of days and weeks. Finally, CMOS technology is capable of fabricating electrodes much smaller than a neuron's soma and dense enough to capture fine details of a single neuron's extracellular field throughout its dendritic tree.

Whether useful information is present at these scales, and whether it can contribute to further understanding of brain function, is an open question. Therefore, in order to address whether ultra-high density *in* vivo electrical recordings will be useful, we collected a series of datasets with an ultra-dense probe during anesthesia from many different brain regions (Figure 3).

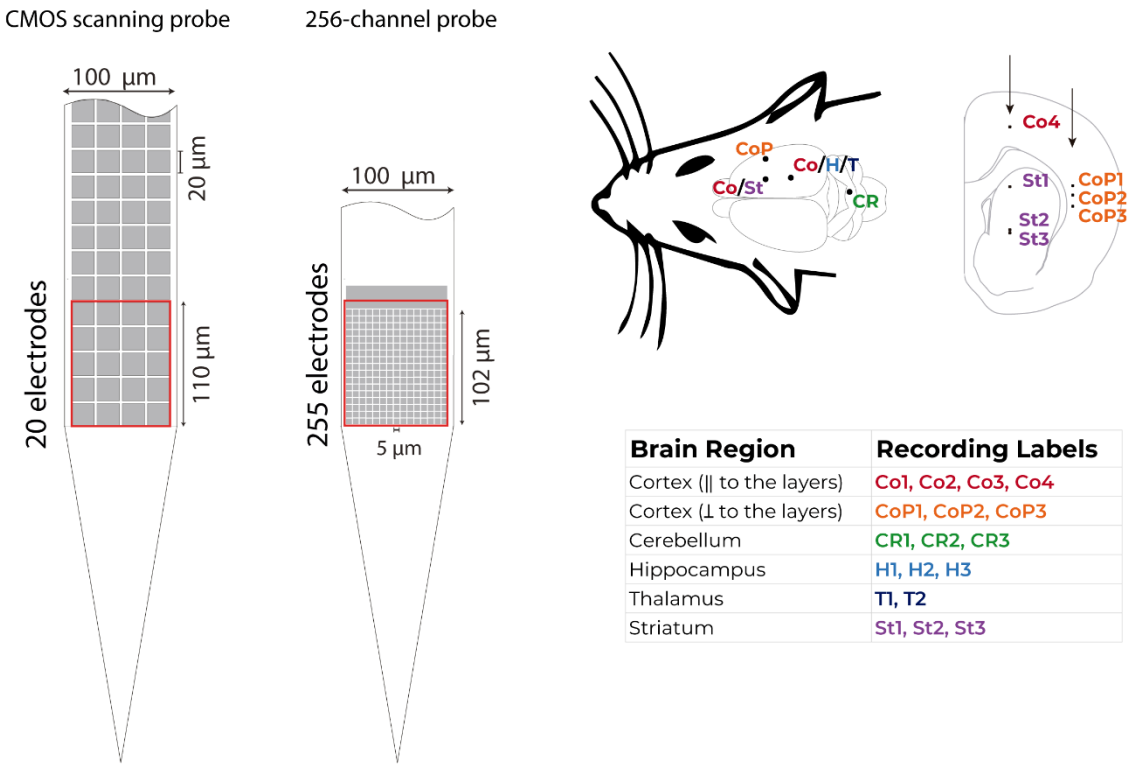

Brain Region	Recording Labels
Cortex (‖ to the layers)	Co1, Co2, Co3, Co4
Cortex (⊥ to the layers)	CoP1, CoP2, CoP3
Cerebellum	CR1, CR2, CR3
Hippocampus	H1, H2, H3
Thalamus	T1, T2
Striatum	St1, St2, St3

Figure 3. The 256-channel ultra-dense probe packs 255 electrodes in the same area (100 x 102 µm) as 20 electrodes from the NeuroSeeker CMOS scanning probe, a 13x increase in density of

electrodes. We conducted four separate penetrations covering six anatomically distinct brain regions and two different orientations with respect to the laminar architecture of cortex, leading to 19 separate recordings.

The ultra-dense probe contains 255 electrodes (and one large reference) with a geometric area of 5 x 5 μm and separated by 1 μm, and was fabricated by IMEC as part of the NeuroSeeker project. The goal of these experiments was to understand at what spatial scale the signals from neighbouring electrodes became redundant (i.e., the extracellular signal becomes spatially over sampled). As shown in Supplementary Figure 3, the probe electrodes have a low impedance value at 1 kHz of 790 ± 100 kOhm. Note that 16 of the 255 electrodes are non-functional because their impedance value at 1kHz is higher than 2 MOhm. The noise magnitude computed in saline for the functional electrodes is 5.09 ± 0.03 μV. The data shown in Supplementary Figure 4 illustrate the ability of this ultra-high-density array of electrodes to detect the activity from the same neuron on several adjacent electrodes. This dataset can be used to explore the optimal electrode configuration (i.e., electrode size and density) required to record and isolate spikes, which may be specific to different brain regions, different neuron types (i.e., different cell sizes and dendritic configurations), and different neuron densities, and thus require ‘‘custom-fit’’ probes for effective neuron isolation (Buzsáki et al. 2015).

Discussion

The NeuroSeeker project is the culmination of a number of efforts to translate major advances in microfabrication into new tools for electrophysiology (Jun et al., 2017b; Lopez et al., 2013; Neves et al., 2008; Raducanu et al., 2017; Torfs et al., 2011). The project has produced a device with multiplexing electrode scanning circuitry within the thin shaft of an implantable neural probe, which provides the highest number of simultaneous outputs for a single shaft *in vivo* extracellular recording device ever achieved.

Here we report that the integrated circuitry of the NeuroSeeker probe do not have an adverse effect on its ability to record neural activity during both acute and chronic recordings. We show that when compared to a passive probe with the same electrode configuration, the NeuroSeeker probe offers simultaneous recordings from >1000 electrodes with similar signal to noise ratio. Given this, we propose that integrating on-shank scanning circuitry is not only a promising technology for creating ultra-high density *in vivo* probes, but will, at the very least, allow the simultaneous recording from the entire probe with a density sufficient for accurate spike sorting.

The number of simultaneously recorded electrodes of the NeuroSeeker probe created new challenges for previously simple aspects of an experiment, e.g. online data review. We also present here a GPU-based method for generating a real-time visualization of the very large data sets generated by such probes. This greatly facilitates the control of an ongoing experiment and provided an intuitive overview of large scale structure present in the spiking activity recorded by the probe, which often spans multiple distinct anatomical and functional brain regions.

Finally, the high costs associated with CMOS development necessitate a large initial investment to produce just a small number of prototype devices. However, the promise of modern CMOS production scaling is that, after an expensive development phase, a large number of equivalent devices can be produced at a tiny fraction of the initial costs. The recent CMOS-based neural probe prototyping efforts, such as NeuroSeeker, have resulted in truly revolutionary devices for

neurophysiology. However, a true revolution in neuroscience will only come when these devices are available in large numbers, to the entire community, for the price of a spool of tungsten wire.

Methods

Animal surgeries

All experiments were conducted with Lister Hooded rats ranging between 400g to 700g of both sexes. For both acute and chronic surgeries, the animals were anesthetized, placed in a stereotaxic frame and undergone a surgical procedure to remove the skin and expose the skull above the targeted brain region. For the acute surgeries we used urethane (1.6g/Kg, IP) anesthesia, while for the chronic ones we used isoflurane gas anesthesia (2% v/v). At the initial stage of each surgery the animal was also injected with atropine (0.05mg/kg), temgesic (20µg/Kg, SC) and rimadyl (5mg/Kg, SC). Small craniotomies (about 1mm in diameter) were performed above the target area. During the surgeries equipment for monitoring the animals' body temperature and a video system for guiding probe insertion (Neto et al. 2016) was used. The targeted insertion coordinates were scaled according to the size of each animal's skull. We measured the distance between bregma (B) and interaural line (IA) for all animals to find the ratio between the animal skull and the reference skull (B – IA = 9 mm) generated as part of the 3D atlas described in (Dimitriadis et al. 2014). Finally, we adapted the insertion coordinates for targeting specific brain regions with the use of the 3D atlas.

Recordings

The CMOS-based probes are assembled on a PCB where the reference (REF) and ground (GND) wires are connected. The recording system consists of a headstage, which configures and calibrates the probe and serializes probe data, a microcoax cable and the base station board with a deserializer chip which connects to a commercial FPGA development board (Xilinx KC705). The computer used for controlling the NeuroSeeker system is connected to the FPGA board via a 1000 kBps-T Ethernet card. This recording system together with the FPGA code and low level C drivers for FPGA – computer communication were developed by IMEC. The FPGA code and the C drivers remain closed source. The protocol for the communication with the low level C drivers for the acquisition and saving of the data and subsequent visualization was implemented in Bonsai. Both Bonsai and the specific NeuroSeeker communication protocol are open source (Bonsai, 2017; Lopes et al., 2015). The CMOS extracellular signals were sampled at 20 kHz with a 10-bit resolution.

Due to the small diameter of the microcoax cable and the size of the behaviour arena there was no requirement for the use of a commutator during the freely moving animal recordings. No cable tension or significant torsion ever developed during the 1-1.5 hour long experimental sessions. The behaviour arena is a 1 x 1 m box with a back projection glass surface as floor onto which a computer projects imagery at a frame rate of 120 Hz. A grasshopper 3 (FLIR) camera is recording the movements of the rat in the arena, also at 120 Hz, while the controlling computer system is live tracking the animal generating x, y positions for each frame. During these recordings the animal was rewarded by small treats randomly thrown into the arena coercing the animal to constantly explore its environment.

For the 256-channel probe recordings we used the Open Ephys (http://www.open-ephys.org/) acquisition board along with two RHD2000 128-channel amplifier boards that amplify and digitally multiplex the extracellular electrodes (Intan Technologies). Extracellular signals in a frequency band

of 0.1–7,500 Hz were sampled at 20 kHz with 16-bit resolution and were saved in a raw binary format for subsequent offline analysis using Bonsai.

Impedance measurements

For the 256-channel probe, impedance tests (at 1 kHz) were performed using a protocol implemented by the RHD2000 series chip (Intan Technologies) with the electrodes placed in a dish with sterile PBS, 1 mM, pH 7.4 and a reference electrode, Ag-AgCl wire (Science Products GmbH, E-255).

Analysis

For the analysis, the CMOS-based probe recordings were filtered with a band-pass of 500-3,500 Hz and they were saved in binary format using a Bonsai interface. When the external reference was selected, to diminish the effect of artefacts shared across all channels, we subtracted the median signal within each group across the recording electrodes from the respective group. For the 256-channel probes, a third order Butterworth filter with a band-pass of 250-9,500 Hz (95% of the Nyquist frequency) was used in the forward-backward mode. The noise magnitude was computed as an estimate of the background noise, σ_{Median} = median(|signal(t)|/0.6745), of each filtered voltage-time trace. Some results were represented as mean ± standard deviation.

References

Berényi, A., Somogyvári, Z., Nagy, A.J., Roux, L., Long, J.D., Fujisawa, S., Stark, E., Leonardo, A., Harris, T.D., and Buzsáki, G. (2014). Large-scale, high-density (up to 512 channels) recording of local circuits in behaving animals. J. Neurophysiol. *111*, 1132–1149.

Blanche, T.J. (2005). Polytrodes: High-Density Silicon Electrode Arrays for Large-Scale Multiunit Recording. J. Neurophysiol. *93*, 2987–3000.

Buzsáki, G., Stark, E., Berényi, A., Khodagholy, D., Kipke, D.R., Yoon, E., and Wise, K.D. (2015). Tools for Probing Local Circuits: High-Density Silicon Probes Combined with Optogenetics. Neuron *86*, 92–105.

Dimitriadis, G., Fransen, A.M.M., and Maris, E. (2014). Sensory and cognitive neurophysiology in rats, Part 1: Controlled tactile stimulation and micro-ECoG recordings in freely moving animals. J. Neurosci. Methods *232*, 63–73.

Dimitriadis, G., Neto, J.P., and Kampff, A.R. (2016). T-SNE visualization of large-scale neural recordings. BioRxiv 1–22.

Du, J., Blanche, T.J., Harrison, R.R., Lester, H.A., and Masmanidis, S.C. (2011). Multiplexed, High Density Electrophysiology with Nanofabricated Neural Probes. PLoS ONE *6*, e26204.

Jun, J., Mitelut, C., Lai, C., Gratiy, S.L., Anastassiou, C.A., and Harris, T.D. (2017a). Real-time spike sorting platform for high-density extracellular probes with ground-truth validation and drift correction. BioRxiv 1–29.

Jun, J.J., Steinmetz, N.A., Siegle, J.H., Denman, D.J., Bauza, M., Barbarits, B., Lee, A.K., Anastassiou, C.A., Andrei, A., Aydın, Ç., et al. (2017b). Fully integrated silicon probes for high-density recording of neural activity. Nature *551*, 232–236.

Kensall, J.J., and Wise, D. (1992). An Implantable CMOS Circuit Interface for Multiplexed Microelectrode Recording Arrays. IEEE J. Solid-State Circuits *27*, 433–443.

Lopes, G., Bonacchi, N., Frazão, J., Neto, J.P., Atallah, B. V, Soares, S., Moreira, L., Matias, S., Itskov, P.M., Correia, P.A., et al. (2015). Bonsai: an event-based framework for processing and controlling data streams. Front. Neuroinformatics *9*, 7.

Lopez, C.M., Andrei, A., Mitra, S., Welkenhuysen, M., Eberle, W., Bartic, C., Puers, R., Yazicioglu, R.F., and Gielen, G. (2013). An implantable 455-active-electrode 52-channel CMOS neural probe. In 2013 IEEE International Solid-State Circuits Conference Digest of Technical Papers, (IEEE), pp. 288–289.

Lopez, C.M., Mitra, S., Putzeys, J., Raducanu, B., Ballini, M., Andrei, A., Severi, S., Welkenhuysen, M., Van Hoof, C., Musa, S., et al. (2016). A 966-electrode neural probe with 384 configurable channels in 0.13µm SOI CMOS. In 2016 IEEE International Solid-State Circuits Conference (ISSCC), (IEEE), pp. 392–393.

Moore-Kochlacs, C.E. (2016). Extracellular electrophysiology with close-packed recording sites: spike sorting and characterization. Boston University.

Najafi, K., and Wise, K.D. (1986). An implantable multielectrode array with on-chip signal processing. IEEE J. Solid-State Circuits *21*, 1035–1044.

Najafi, K., Wise, K.D., and Mochizuki, T. (1985). A high-yield IC-compatible multichannel recording array. IEEE Trans. Electron Devices *32*, 1206–1211.

Neto, J.P., Lopes, G., Frazão, J., Nogueira, J., Lacerda, P., Baião, P., Aarts, A., Andrei, A., Musa, S., Fortunato, E., et al. (2016). Validating silicon polytrodes with paired juxtacellular recordings: method and dataset. J. Neurophysiol. *116*, 892–903.

Neves, H.P., Torfs, T., Yazicioglu, R.F., Aslam, J., Aarts, A.A., Merken, P., Ruther, P., and Van Hoof, C. (2008). The NeuroProbes project: a concept for electronic depth control. Conf. Proc. Annu. Int. Conf. IEEE Eng. Med. Biol. Soc. IEEE Eng. Med. Biol. Soc. Annu. Conf. *2008*, 1857.

Obien, M.E.J., Deligkaris, K., Bullmann, T., Bakkum, D.J., and Frey, U. (2015). Revealing neuronal function through microelectrode array recordings. Front. Neurosci. *8*, 423.

Raducanu, B.C., Yazicioglu, R.F., Lopez, C.M., Ballini, M., Putzeys, J., Wang, S., Andrei, A., Welkenhuysen, M., Van Helleputte, N., Musa, S., et al. (2016). Time multiplexed active neural probe with 678 parallel recording sites. In European Solid-State Device Research Conference, (IEEE), pp. 385–388.

Raducanu, B.C., Yazicioglu, R.F., Lopez, C.M., Ballini, M., Putzeys, J., Wang, S., Andrei, A., Rochus, V., Welkenhuysen, M., Helleputte, N. van, et al. (2017). Time Multiplexed Active Neural Probe with 1356 Parallel Recording Sites. Sensors *17*, 2388.

Rios, G., Lubenov, E. V., Chi, D., Roukes, M.L., and Siapas, A.G. (2016). Nanofabricated Neural Probes for Dense 3-D Recordings of Brain Activity. Nano Lett. *16*, 6857–6862.

Rossant, C., Kadir, S.N., Goodman, D.F.M., Schulman, J., Belluscio, M., Buzsaki, G., and Harris, K.D. (2015). Spike sorting for large, dense electrode arrays (Cold Spring Harbor Labs Journals).

Ruther, P., and Paul, O. (2015). New approaches for CMOS-based devices for large-scale neural recording. Curr. Opin. Neurobiol. *32*, 31–37.

Scholten, K., and Meng, E. (2016). Electron-beam lithography for polymer bioMEMS with submicron features. Microsyst. Nanoeng. *2*, 16053.

Scholvin, J., Kinney, J.P., Bernstein, J.G., Moore-Kochlacs, C., Kopell, N., Fonstad, C.G., and Boyden, E.S. (2016). Close-packed silicon microelectrodes for scalable spatially oversampled neural recording. IEEE Trans. Biomed. Eng. *63*, 120–130.

Seymour, J.P., Wu, F., Wise, K.D., and Yoon, E. (2017). State-of-the-art MEMS and microsystem tools for brain research. Microsyst. Nanoeng. *3*, 16066.

Shobe, J.L., Claar, L.D., Parhami, S., Bakhurin, K.I., and Masmanidis, S.C. (2015). Brain activity mapping at multiple scales with silicon microprobes containing 1024 electrodes. J. Neurophysiol. *114*, 2043–2052.

Steinmetz, N.A. (2016). NeuroPixel project.

Stevenson, I. (2017). Tracking Advances in Neural Recording.

Stevenson, I.H., and Kording, K.P. (2011). How advances in neural recording affect data analysis. Nat. Neurosci. *14*, 139–142.

Torfs, T., Aarts, A. a. A., Erismis, M.A., Aslam, J., Yazicioglu, R.F., Seidl, K., Herwik, S., Ulbert, I., Dombovari, B., Fiath, R., et al. (2011). Two-dimensional multi-channel neural probes with electronic depth control. IEEE Trans. Biomed. Circuits Syst. *5*, 403–412.

Wise, K.D., and Najafi, K. (1991). Microfabrication techniques for integrated sensors and microsystems. Science *254*, 1335–1342.